

Origin of giant wave ripples in snowball Earth cap carbonate

Michael P. Lamb^{1*}, Woodward W. Fischer¹, Timothy D. Raub^{1,2}, J. Taylor Perron³, and Paul M. Myrow⁴

¹Division of Geological and Planetary Sciences, California Institute of Technology, Pasadena, California 91125, USA

²Department of Earth Sciences, University of St. Andrews, St. Andrews KY16 9AL, UK

³Department of Earth, Atmospheric, and Planetary Sciences, Massachusetts Institute of Technology, Cambridge, Massachusetts 02139, USA

⁴Department of Geology, Colorado College, Colorado Springs, Colorado 80903, USA

ABSTRACT

The most extreme climate transitions in Earth history are recorded by the juxtaposition of Neoproterozoic glacial deposits with overlying cap carbonate beds. Some of the most remarkable sedimentary structures within these beds are sharp-crested (trochoidal) bedforms with regular spacing of as much as several meters that are often interpreted as giant wave ripples formed under extreme wave conditions in a nonuniform postglacial climate. Here we evaluate this hypothesis using a new bedform stability diagram for symmetric oscillatory flows that indicates that the first-order control on the formation of trochoidal rather than hummocky bedforms is sediment size, not wave climate. New measurements of bedform wavelengths and particle sizes from the ca. 635 Ma Nuccaleena Formation, Australia, indicate that the giant ripples are generally composed of coarse to very coarse sand; most are within the trochoidal bedform stability phase space for normal wave climates. Moreover, numerical simulations of flow over fixed bedforms show that symmetric trochoidal ripples with a nearly vertical angle of climb may be produced over long time periods with variable wave climates in conjunction with rapid seabed cementation. These data reveal that, rather than extreme wave conditions, the giant wave ripples are a consequence of the unusual mode of carbonate precipitation during a global carbon cycle perturbation unprecedented in Earth history.

INTRODUCTION

Neoproterozoic ice ages and subsequent postglacial hothouses mark the most extreme climates in Earth history (e.g., Kirschvink, 1992). Weathering fluxes, primary productivity, and the carbon cycle were severely perturbed during these intervals (e.g., Hoffman et al., 1998), and the physical stratigraphic record of snowball Earth deglaciation is correspondingly exceptional, particularly of the late Neoproterozoic Marinoan event (e.g., Kennedy, 1996). In many localities, meter- to decameter-thick cap carbonate units spanning the ca. 635 Ma terminal deglacial to early postglacial transition feature 1–4 strata-bounded sets of long, regularly spaced (~1–6 m wavelength), symmetric cusped sedimentary structures (Fig. DR1 in the GSA Data Repository¹), referred to as trochoidal bedforms. Although a number of origins have been proposed (e.g., James et al., 2001), the leading hypothesis is that these strata are the result of wave ripples (e.g., Allen and Hoffman, 2005a; Jerolmack

and Mohrig, 2005), albeit at a size substantially larger than most modern examples.

Allen and Hoffman (2005a) inferred that the giant ripples formed under extremely large waves (wave periods, $T = 21$ – 30 s; wave heights, $H > 7.5$ – 12 m) that transported sediment in water depths of $h = 200$ – 400 m, a scenario unlike any wave conditions in modern ocean basins. Jerolmack and Mohrig (2005) countered that this interpretation may constitute one of many valid reconstructions, but did not consider the trochoidal ripple morphology, which Allen and Hoffman (2005b) contended requires extreme wave conditions. The heart of this debate revolves around assumptions used to invert geologic data, in particular the conditions under which trochoidal ripples form. Herein we develop a new stability diagram for large-scale bedforms developed under oscillatory flow and show that cap carbonate giant wave ripples are expected to have formed under normal wave conditions, given their coarse sediment sizes. Our findings have significant implications for reconstructing paleoenvironmental conditions from large-scale wave ripples, in particular during the Neoproterozoic, when climate extremes and diversification of multicellular life were extraordinary (e.g., Hoffman and Li, 2009; Pierrehumbert et al., 2011).

OSCILLATORY BEDFORM STABILITY

Our new bedform stability diagram is based in part on an exhaustive compilation by Pedocchi and Garcia (2009) that highlights, for purely oscillatory flow, a robust boundary separating

large two-dimensional (2-D) trochoidal bedforms from hummocky bedforms as $U_o = 25w_s$, where U_o is the near-bed maximum wave orbital velocity and w_s is the particle settling velocity. Given this constraint and an orbital diameter, the stability-field boundary can be inferred from a unique combination of grain size and wave period (or orbital velocity, equivalently) (Fig. 1A). The orbital velocity is directly related to the near-bed orbital diameter, d_o , by definition (i.e., $d_o = U_o T / \pi$) and orbital diameter scales with bedform wavelength, λ , for large orbital bedforms following $\lambda = C_1 d_o$, where $C_1 = 0.65$ (e.g., Pedocchi and Garcia, 2009). To complete the bedform-stability phase space, we calculate the boundary for incipient sediment motion following You and Yin (2006), and for upper plane bed as $\tau_* \approx 3$ (where τ_* is the Shields number) based on our reanalysis of experimental data in purely oscillatory flow (Dumas et al., 2005; Cummings et al., 2009). Results for a typical example case where $d_o = 3.07$ m (i.e., $\lambda = 2$ m) show that, for wave conditions comparable to modern observations during fair weather and storms (i.e., $T < \sim 15$ s), bedforms are expected to be hummocky for grain sizes $D < 0.2$ mm, approximately equivalent to fine sand and finer, or alternatively, the bed state is predicted to be planar (Fig. 1A). For the same wave conditions, trochoidal bedforms occur for $D > 0.5$ mm (coarse sand and coarser) except under very small wave periods (i.e., $T < 5$ s) where hummocks can develop.

Although experiments using oscillatory ducts can reproduce the entire parameter space in Figure 1A, the same is not true for surface gravity waves in the world's oceans, which have physical limits. The shortest wave period corresponds to waves that are just steep enough to break (Muir Wood, 1969), $H/L > 0.142 \tanh(2\pi h/L)$, where H is wave height, L is the wavelength, and h is water depth (Fig. 1B). The longest possible period for waves of a given height is $T = C_2 2\pi U_w / g = 2\pi C_2 \sqrt{H/C_3 g}$ (where g is gravitational acceleration, and $C_2 = 1.5$ and $C_3 = 0.3$ are empirical coefficients), based on observations of fetch-unlimited conditions that span orders of magnitude in wind velocity (Bretshneider, 1959). These two bounds, along with Airy wave theory and a constraint on bedform wavelength, define the conditions under which wind-driven surface gravity waves produce symmetric oscillatory flow (Fig. 1B).

*E-mail: mpl@gps.caltech.edu.

¹GSA Data Repository item 2012236, Table DR1 (Neoproterozoic wave ripple sediment sizes and wavelengths), Figure DR1 (photograph of giant wave ripple), Figure DR2 (bedform stability diagram for siliclastic grains and modern ocean conditions), and G33093_Matlab_Codes.zip (Matlab codes to calculate wave hydrodynamics and generate paleohydraulic reconstructions), is available online at www.geosociety.org/pubs/ft2012.htm, or on request from editing@geosociety.org or Documents Secretary, GSA, P.O. Box 9140, Boulder, CO 80301, USA.

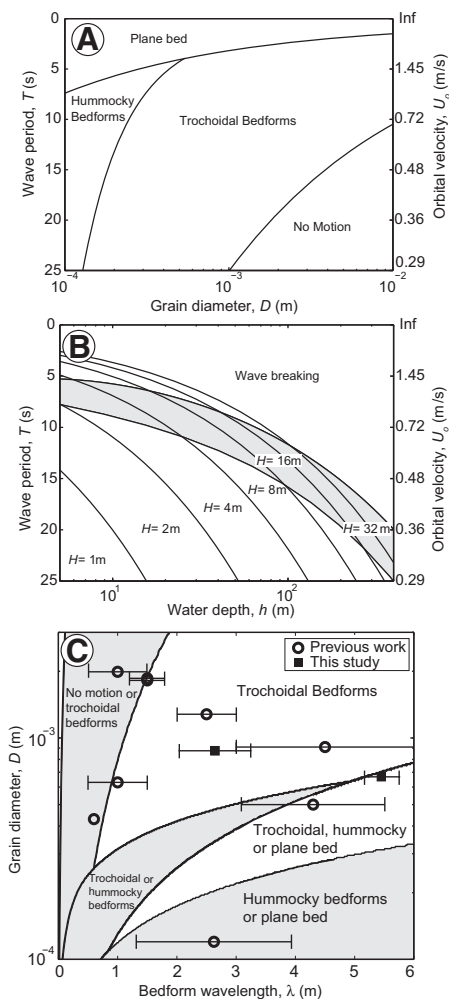


Figure 1. A: Bedform stability fields as function of wave period, near-bed orbital velocity, and grain diameter for 2-m-wavelength bedforms. Bed stress is calculated from Grant and Madsen (1982), where bed roughness is $2.5D$ (D is particle size), kinematic fluid viscosity is $7 \times 10^{-5} \text{ m}^2/\text{s}$ (i.e., seawater at 35°C ; cf. Finnegan et al., 2011), and submerged specific density of sediment is $R = 1.78$, which corresponds to particle density of 2840 kg/m^3 (i.e., carbonate) and fluid density for seawater at 35°C of 1022 kg/m^3 . **B: Corresponding wave heights (H) and water depths (h) necessary to produce given wave period and near-bed orbital velocity combination according to Airy wave theory for symmetrical oscillatory flow.** Shaded region marks zone of observed linear waves (Bretshneider, 1959; Muir Wood, 1969). **C: Bedform stability diagram for linear oscillatory waves as function of grain diameter and bedform wavelength using same parameters as in A.** Ambiguity in stability boundaries reflects uncertainty in water depth ($1 < h < 100 \text{ m}$) and wave climate (B). Horizontal error bars represent full range of observed bedform wavelengths (Table DR1; see footnote 1). Some bedforms (e.g., hummocks, plane bed) may occur outside of our solution space, for example, in surf zone where waves are asymmetric and nonlinear, which may explain origin of some hummocky cross-stratified grainstones (e.g., Hoffman et al., 1998). Comparison stability diagrams for modern ocean temperatures and siliclastic grains as well as source codes to reproduce these diagrams are given in the Data Repository (see footnote 1).

To perform a reconstruction, we require information on water depth, bedform wavelength, and sediment size (Figs. 1A and 1B). Water depth is the most difficult parameter to characterize from ancient deposits, and therefore we fold this uncertainty into the bedform stability diagram by recasting it in terms of sediment diameter and bedform wavelength (Fig. 1C), allowing for the full range of shelf water depths ($h < 100 \text{ m}$; Fig. 1B). Thus, for some combinations of sediment size and bedform wavelength, multiple bed states are possible given the range of possible wave periods (or orbital velocities) observed for $h < 100 \text{ m}$. This stability diagram (Fig. 1C) reconciles long-standing debates concerning the origin of large-scale oscillatory bedforms (e.g., Swift et al., 1983; Quin, 2011) and indicates that large trochoidal bedforms are favored for $D > \sim 0.5 \text{ mm}$, whereas hummocky bedforms dominate the phase space for fine sand and very fine sand ($D < 0.2 \text{ mm}$), regardless of wave climate and water depth. These predictions are supported by observations that meter-scale hummocky cross stratification occurs almost exclusively in fine and very fine sand (e.g., Dott and Bourgeois, 1982; Myrow et al., 2008), and that large 2-D trochoidal ripples

typically occur in coarse sand and gravel (e.g., Leckie, 1988; Cummings et al., 2009).

NEOPROTEROZOIC GIANT WAVE RIPPLES

Our bedform stability model is similar to that used for paleohydraulic reconstruction of Neoproterozoic giant wave ripples by Allen and Hoffman (2005a); however, they assumed that trochoidal ripples form only at the threshold for sediment motion. Allen and Hoffman (2005a) reported $D = 0.12 \text{ mm}$ for giant ripples in the Mackenzie Mountains (Canada), and the threshold condition for this sediment size yields extremely large wave periods ($T > 30 \text{ s}$) (e.g., Fig. 1A), and consequently extremely large water depths ($h > 400 \text{ m}$) and wave heights ($H > 20 \text{ m}$) (e.g., Fig. 1B).

A more plausible alternative to invoking extreme wave conditions is that the ripples formed under normal wave conditions, but in relatively coarse sediment (Fig. 1C). Bedform wavelengths are readily measured in outcrop, but measuring sediment diameters in diagenetically stabilized dolostone lithologies is more difficult. We compiled data from previous studies that reported measurements of wavelength

and sediment size from large 2-D trochoidal wave ripples in Neoproterozoic cap carbonate deposits (Table DR1 in the Data Repository). To supplement these data, we measured bedform wavelengths and grain sizes from several ca. 635 Ma Australian cap dolostone units equivalent to the Nuccaleena Formation (Raub et al., 2007) that contain large trochoidal wave ripples. Bedform wavelengths were measured directly on dip slope-exposed bedding planes in the field, perpendicular to ripple axes. Sediment sizes were measured in thin section by transmitted-light and reflected-light microscopy, often using a white-card method (e.g., Zenger, 1979) to reveal relict grain textures in the recrystallized dolostone (Fig. 2).

The data show large mean sediment diameters ($D > 0.5 \text{ mm}$) with clear examples of very coarse sand ($D = 1\text{--}2 \text{ mm}$) (Table DR1), consistent with common reports of macropeloids in cap carbonate beds preserved elsewhere (e.g., James et al., 2001; Hoffman and Schrag, 2002). Given the observed bedform wavelengths, this places all but one of the observations in the predicted zone for trochoidal bedforms or in ambiguous domains of the solution space (Fig. 1C). Consequently, we conclude that large trochoidal ripples in snowball Earth cap carbonate beds are best explained by formation under normal wave conditions, and that a postglacial climate characterized by extreme sustained winds (e.g., Hoffman and Li, 2009) or heightened hurricane intensity (e.g., Pierrehumbert et al., 2011) is not necessary.

DISCUSSION

If the giant wave ripples common to Marinoan cap carbonate deposits can be explained by normal wave climates given the observed coarse particle sizes, then why are these bedforms, which are abundant following the ca. 635 Ma deglaciation, not more common in the sedimentary record? We hypothesize that the answer is tied to the unique style of carbonate precipitation and deposition associated with Marinoan cap carbonate. In siliclastic environments, large grains are rarely transported far from shore, and, with the exception of ravinement surfaces, most shelves are dominated by fine sand and mud; thus hummocky bedforms are associated with normal storm waves at shelfal depths (Fig. 1C) (e.g., Swift et al., 1983; Passchier and Kleinhans, 2005). Carbonate-rich settings do not have the same limitation because large grains can be produced in situ (or nearby), particularly after the evolution of animal and algal skeletons.

In addition to coarse grains, one of the most striking features of the cap carbonate giant wave ripples is a near-vertical direction of climb (Fig. DR1) (Allen and Hoffman, 2005a). This seems to imply formation under a steady wave climate, because nearly symmetrical waves

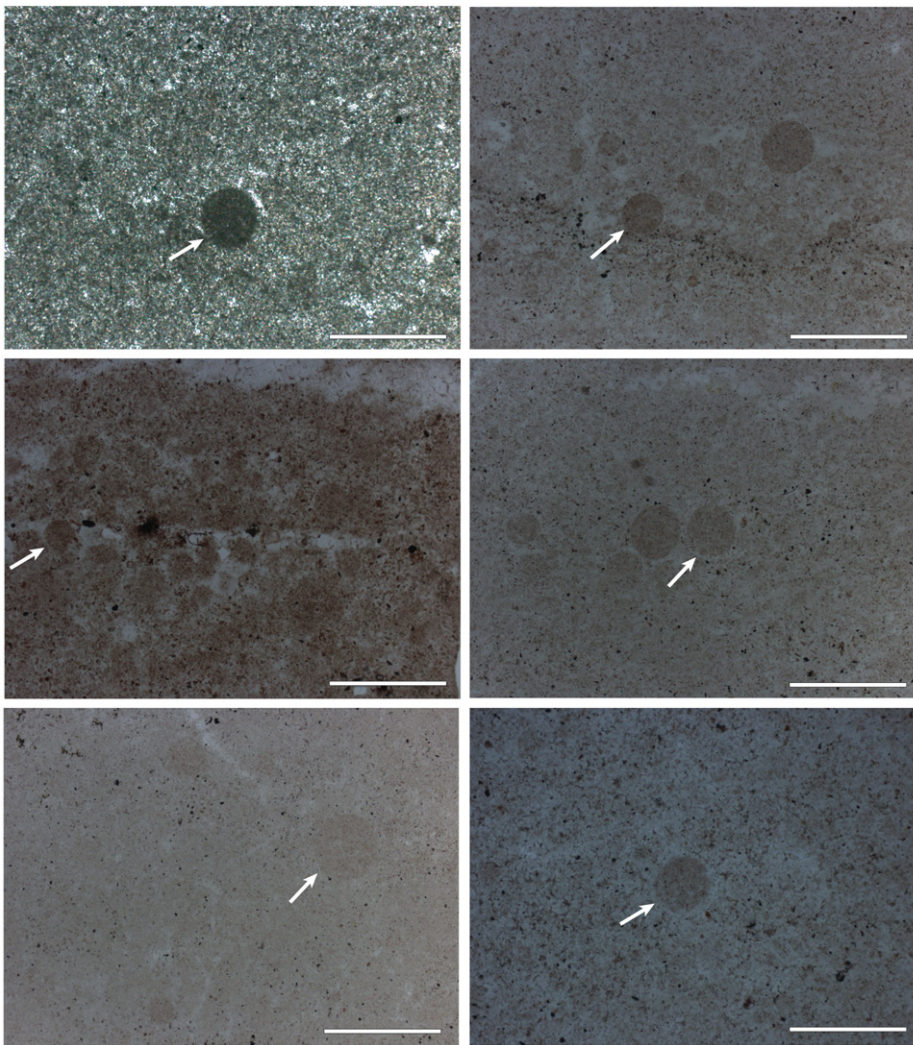


Figure 2. Photomicrographs of rare preserved grains within recrystallized giant-ripple horizons from Nuccaleena Formation (Australia) cap dolostone. White bars mark 1 mm scale bar, and white arrows indicate example grain boundary; other large preserved grains also are apparent in images. Note spherical nature of grains, suggesting low porosity and bulk density typical of carbonate rock, which was assumed to generate Figure 1.

are required to avoid net crest migration and preservation of dune-scale cross-stratification (e.g., Arnott and Southard, 1990). Although preferential north-south orientations of ripple crests suggest zonal winds (Hoffman and Li, 2009), it seems unlikely that fair-weather wave base was consistently more than an order of magnitude deeper than today and that wave climate remained exactly the same, even with zonal winds, over the time required to produce thick (0.5–2 m) ripple-laminated deposits at many locations globally. A similar problem exists if these deposits are to be explained by multiple storm events, and formation during a single storm event seems unlikely given the extremely high deposition rates that would be required (Jerolmack and Mohrig, 2005). Moreover, correlatable paleomagnetic reversals in cap carbonate units, including those studied here, suggest that these structures developed

over long periods of time (>10 k.y.) (Trindade et al., 2003; Raub et al., 2007).

Our preferred scenario is that once initially generated in coarse sediment, the wave ripples were cemented in place, or stabilized by slack-water deposits, and morphodynamic feedbacks maintained the bedform shape under incremental deposition separated by potentially long intervals of inactivity. This is consistent with evidence for seafloor carbonate precipitation during genesis of the Marinoan cap carbonates (James et al., 2001; Hoffman and Schrag, 2002). To test the viability of this hypothesis, we simulated flow over a fixed ripple bedform using a numerical model (Fig. 3A). Results show a strong negative spatial gradient in time-averaged near-bed shear stress immediately to the lee of the ripple crest, which should cause sediment deposition (Fig. 3B). We systematically decreased the near-bed orbital diameter

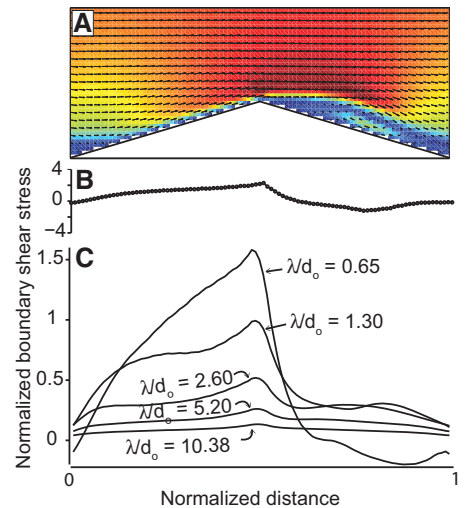


Figure 3. Numerical simulation of two-dimensional sinusoidal oscillatory flow over giant ripple with steepness of 0.15. **A:** Example velocity field from simulation with $\lambda/d_o = 0.65$ (i.e., the equilibrium case), showing separation in lee of ripple crest (see text). Lengths of velocity vectors are proportional to magnitude of velocity. Linear color scale reflects relative velocity magnitude. Boundary conditions were free slip at upper boundary, no slip at bed, and periodic on side boundaries. Time-dependent velocity field was calculated with lattice Boltzmann method for turbulent flow (Reynolds numbers ranging from 10^4 to 3×10^5) using large-eddy closure (e.g., Aidun and Clausen, 2010). **B:** Normalized boundary shear stress (dimensionless) at instant shown in A. **C:** Normalized, time-averaged boundary shear stress (dimensionless) for five simulations with different values of λ/d_o . Stress is averaged over half wave cycle in which mean flow is to right.

from that predicted to be in equilibrium with the ripple wavelength ($\lambda/d_o = 0.65$) to flows with λ/d_o ranging from 1.30 to 10.38. A comparison of the stress profiles (Fig. 3C) reveals that simulations with d_o different from the equilibrium case have a similar form, including the important characteristic that the steepest shear stress gradient is in the lee of the ripple crest. Thus, depositional patterns during transport events may have mimicked the inherited topography of the cemented or stabilized bed despite changes in wave conditions and potentially even changes in sediment-size inputs.

CONCLUSIONS

Bedform stability relationships for purely oscillatory flow show that large ($\lambda > 1$ m) trochoidal ripples form in relatively coarse sediment (medium to coarse sand and coarser), whereas large hummocky bedforms require finer sediment, generally fine to very fine sand. Given the coarse sediment that composes cap carbonate giant wave ripples, the trochoidal bedforms are best explained as a result of normal wave climates without extreme winds

or enhanced hurricanes. Instead, the important aspects of cap carbonate deposition that facilitated synthesis of these large bedforms were (1) production of large grains directly on the shelf (either produced in situ or drowned during post-glacial transgression) that allowed the stability of trochoidal ripples, and (2) high syndepositional cementation rates that allowed aggradation and preservation of these features. These anomalous carbonate deposition regimes must have been globally common, but regionally and temporally variable, since wave-ripple horizons within individual cap carbonate units are discrete. Thus, giant wave ripples are part and parcel of a larger suite of structures (e.g., Hoffman and Schrag, 2002) that point to significant perturbations of the carbon cycle that are unlike any other interval in Earth history.

ACKNOWLEDGMENTS

Lamb acknowledges support from the donors of the American Chemical Society Petroleum Research Fund. Fischer acknowledges support from the Agouron Institute. Raub was supported by National Science Foundation grant EAR-0739105. We thank Tony Prave, John Southard, and Paul Hoffman for informal reviews and delightful discussions. David Mohrig and Bob Dalrymple provided formal reviews that strengthened the final manuscript.

REFERENCES CITED

- Aidun, C.K., and Clausen, J.R., 2010, Lattice-Boltzmann method for complex flows: *Annual Review of Fluid Mechanics*, v. 42, p. 439–472, doi:10.1146/annurev-fluid-121108-145519.
- Allen, P., and Hoffman, P., 2005a, Palaeoclimatology—Formation of Precambrian sediment ripples: *Nature*, v. 436, p. E1–E2, doi:10.1038/nature04026.
- Allen, P.A., and Hoffman, P.F., 2005b, Extreme winds and waves in the aftermath of a Neoproterozoic glaciation: *Nature*, v. 433, p. 123–127, doi:10.1038/nature03176.
- Arnott, R.W., and Southard, J.B., 1990, Exploratory flow-duct experiments on combined-flow bed configurations, and some implications for interpreting storm-event stratification: *Journal of Sedimentary Petrology*, v. 60, p. 211–219, doi:10.1306/212F9156-2B24-11D7-8648000102C1865D.
- Bretshneider, C.L., 1959, Wave variability and wave spectra for wind-generated gravity waves: U.S. Army Corps of Engineers Beach Erosion Board Technical Memo 118, 192 p.
- Cummings, D.I., Dumas, S., and Dalrymple, R.W., 2009, Fine-grained versus coarse-grained wave ripples generated experimentally under large-scale oscillatory flow: *Journal of Sedimentary Research*, v. 79, p. 83–93, doi:10.2110/jsr.2009.012.
- Dott, R.H., and Bourgeois, J., 1982, Hummocky stratification: Significance of its variable bedding sequences: *Geological Society of America Bulletin*, v. 93, p. 663–680, doi:10.1130/0016-7606(1982)93<663:HSSOIV>2.0.CO;2.
- Dumas, S., Arnott, R.W.C., and Southard, J.B., 2005, Experiments on oscillatory-flow and combined-flow bed forms: Implications for interpreting parts of the shallow-marine sedimentary record: *Journal of Sedimentary Research*, v. 75, p. 501–513, doi:10.2110/jsr.2005.039.
- Finnegan, S., Bergmann, K., Eiler, J.M., Jones, D.S., Fike, D.A., Eisenman, I., Hughes, N.C., Tripathi, A.K., and Fischer, R.W.C., 2011, The magnitude and duration of Late Ordovician–Early Silurian glaciation: *Science*, v. 331, p. 903–906, doi:10.1126/science.1200803.
- Grant, W.D., and Madsen, O.S., 1982, Movable bed roughness in unsteady oscillatory flow: *Journal of Geophysical Research*, v. 87, p. 469–481, doi:10.1029/JC087iC01p00469.
- Hoffman, P.F., and Li, Z.-X., 2009, A palaeogeographic context for Neoproterozoic glaciation: *Palaeogeography, Palaeoclimatology, Palaeoecology*, v. 277, p. 158–172, doi:10.1016/j.palaeo.2009.03.013.
- Hoffman, P.F., and Schrag, D.P., 2002, The snowball Earth hypothesis: Testing the limits of global change: *Terra Nova*, v. 14, p. 129–155, doi:10.1046/j.1365-3121.2002.00408.x.
- Hoffman, P.F., Kaufman, A.J., Halverson, G.P., and Schrag, D.P., 1998, A Neoproterozoic snowball earth: *Science*, v. 281, p. 1342–1346, doi:10.1126/science.281.5381.1342.
- James, N.P., Narbonne, G.M., and Kyser, T.K., 2001, Late Neoproterozoic cap carbonates: Mackenzie Mountains, northwestern Canada: Precipitation and global glacial meltdown: *Canadian Journal of Earth Sciences*, v. 38, p. 1229–1262, doi:10.1139/e01-046.
- Jerolmack, D.J., and Mohrig, D., 2005, Palaeoclimatology: Formation of Precambrian sediment ripples: *Nature*, v. 436, p. E1–E2, doi:10.1038/nature04025.
- Kennedy, M.J., 1996, Stratigraphy, sedimentology, and isotopic geochemistry of Australian Neoproterozoic postglacial cap dolostones: Deglaciation, $\delta^{13}\text{C}$ excursions, and carbonate precipitation: *Journal of Sedimentary Research*, v. 66, p. 1050–1064, doi:10.1306/D42684A5-2B26-11D7-8648000102C1865D.
- Kirschvink, J.L., 1992, Late Proterozoic low-latitude glaciation: The snowball Earth, in Schopf, J.W., and Klein, C., eds., *The Proterozoic biosphere*: Cambridge, UK, Cambridge University Press, p. 51–52.
- Leckie, D., 1988, Wave-formed, coarse grained ripples and their relationship to hummocky cross-stratification: *Journal of Sedimentary Petrology*, v. 58, p. 607–622, doi:10.1306/212F8E04-2B24-11D7-8648000102C1865D.
- Muir Wood, A.M., 1969, *Coastal hydraulics*: London, UK, MacMillan, 288 p.
- Myrow, P.M., Lukens, C., Lamb, M.P., Houck, K., and Strauss, J., 2008, Dynamics of a transgressive prodeltaic system: Implications for geography and climate within a Pennsylvanian intracratonic basin, Colorado, USA: *Journal of Sedimentary Research*, v. 78, p. 512–528, doi:10.2110/jsr.2008.061.
- Passchier, S., and Kleinhans, M.G., 2005, Observations of sand waves, megaripples, and hummocks in the Dutch coastal area and their relation to currents and combined flow conditions: *Journal of Geophysical Research*, v. 110, F04S15, doi:10.1029/2004JF000215.
- Pedocchi, F., and Garcia, M.H., 2009, Ripple morphology under oscillatory flow: 1. Prediction: *Journal of Geophysical Research*, v. 114, C12014, doi:10.1029/2009jc005354.
- Pierrehumbert, R.T., Abbot, D.S., Voigt, A., and Koll, D., 2011, Climate of the Neoproterozoic: *Annual Review of Earth and Planetary Sciences*, v. 39, p. 417–460, doi:10.1146/annurev-earth-040809-152447.
- Quin, J.G., 2011, Is most hummocky cross-stratification formed by large-scale ripples?: *Sedimentology*, v. 58, p. 1414–1433, doi:10.1111/j.1365-3091.2010.01219.x.
- Raub, T.D., Evans, D.A.D., and Smirnov, A.V., 2007, Siliciclastic prelude to Elatina-Nuccaleena deglaciation: Lithostratigraphy and rock magnetism of the base of the Ediacaran system, in Vickers-Rich, P., and Komarower, P., eds., *The rise and fall of the Ediacaran biota*: Geological Society of London Special Publication 286, p. 53–76, doi:10.1144/SP286.5.
- Swift, D.J., Figueiredo, A.G., Freeland, G.L., and Oertel, G.F., 1983, Hummocky cross-stratification and megaripples: A geological double standard?: *Journal of Sedimentary Petrology*, v. 53, p. 1295–1317.
- Trindade, R.I.F., Font, E., D'Agrella, M.S., Nogueira, A.C.R., and Riccomini, C., 2003, Low-latitude and multiple geomagnetic reversals in the Neoproterozoic Puga cap carbonate, Amazon craton: *Terra Nova*, v. 15, p. 441–446, doi:10.1046/j.1365-3121.2003.00510.x.
- You, Z.-J., and Yin, B., 2006, A unified criterion for initiation of sediment motion and inception of sheet flow under water waves: *Sedimentology*, v. 53, p. 1181–1190, doi:10.1111/j.1365-3091.2006.00810.x.
- Zenger, D.H., 1979, Primary textures in dolostones and recrystallized limestones; a technique for their microscopic study; discussion: *Journal of Sedimentary Petrology*, v. 49, p. 677–678, doi:10.1306/212F781A-2B24-11D7-8648000102C1865D.

Manuscript received 6 December 2011

Revised manuscript received 26 March 2012

Manuscript accepted 2 April 2012

Printed in USA